Carbohydrate Polymers 83 (2011) 653–658

Contents lists available at ScienceDirect

Carbohydrate Polymers

journal homepage: www.elsevier.com/locate/carbpol

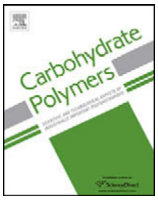

Preparation of chitosan/graphene oxide composite film with enhanced mechanical strength in the wet state

Donglin Han, Lifeng Yan*, Wufeng Chen, Wan Li

Hefei National Laboratory for Physical Sciences at the Microscale and Department of Chemical Physics, and Anhui Province Key Laboratory of Biomass Clean Energy, University of Science and Technology of China, Hefei 230026, PR China

ARTICLE INFO

Article history:
Received 13 July 2010
Received in revised form 12 August 2010
Accepted 13 August 2010
Available online 20 August 2010

Keywords:
Chitosan
Graphene oxide
Composite film
Strength

ABSTRACT

Chitosan/graphene oxide composite films have been prepared by the mixing aqueous solution of chitosan and graphene oxide in the present of diluted acetic acid. The structure, thermal stability and mechanical properties of the composite films have been investigated by the wide-angle X-ray diffraction, Fourier transform infrared spectroscopy, scanning electron microscopy, atomic force microscopy, thermogravimetry analysis, and mechanical test. The results obtained from those different studies revealed that chitosan and graphene oxide could mix with each other homogeneously and the mechanical properties of the as-prepared films were improved significantly over that of the pure chitosan film, especially at wet state. The tensile strength of the film of chitosan/graphene oxide (5:1, w/w) is 1.7 times higher than that of the pure chitosan film at dry state while it is 3 times higher at wet state. In addition, the composite films also showed a high storage modulus up to 200 °C. The composite films have potential application as biomaterials or packing materials.

© 2010 Elsevier Ltd. All rights reserved.

1. Introduction

Graphene, a single layer of carbon atoms in a hexagonal lattice, has recently attracted much attention due to its novel electronic and mechanical properties (Ramanathan et al., 2008). Graphene is usually prepared by the reduction of its precursor graphene oxide (Chen, Yan, & Bangal, 2010), a typical pseudo-two-dimensional oxygen-containing solid in bulk form, possesses functional groups including hydroxyls, epoxides, and carboxyls (McAllister et al., 2007; Niyogi et al., 2006; Stankovich et al., 2007; Vickery, Patil, & Mann, 2009). Both graphene and graphene oxide papers show very high mechanical properties with well biocompatibility, and they have potential application as biomaterials (Stankovich et al., 2006; Wakabayashi et al., 2008; Wang, Tambraparni, Qiu, Tipton, & Dean, 2009). The chemical groups of graphene oxide have been found to be a feasible and effective means of improving the dispersion of graphene. Additionally, functional side groups bound to the surface of graphene oxide or graphene sheets may improve the interfacial interaction between graphene oxide/graphene and the matrix similarly to that observed for functionalized carbon nanotube-based nanocomposites (Coleman et al., 2004). Thus, by combining remarkable mechanical properties and low costs, 2D graphene or graphene oxide sheets are expected to offer promising nanoscale filler for the next generation of nanocomposite materials. In particular, some prominent reports have explored the intriguing applications (such as organic conductive films and heat-resistant material) of graphene oxide–polymer nanocomposites (Fang, Wang, Lu, Yang, & Nutt, 2009; Kong, Yoo, & Jung, 2009). Since graphene oxide can be dispersed at the individual sheet level in water, it is possible to achieve a truly molecular-level dispersion of graphene oxide if water is used as the common solvent for both graphene oxide and the polymer matrix. In addition, it has been reported that the epoxy groups in graphene oxide favor to react with primary amine group by addition, which has been widely used to modify graphene oxide. So it is possible to form a new mixture of chitosan and graphene oxide through the special interaction beside the H-bondings between them.

We report here a simple and environmental benign preparation of chitosan/graphene oxide composite films by blending graphene oxide into the chitosan matrix using diluted acetic acid as the processing solvent.

2. Experimental

2.1. Materials

Chitosan was obtained from Sinopharm Chemical Reagent Co. Ltd. in China (degree of deacetylation: 88%, $M_w = 8000–20{,}000$) as a matrix material. Graphite powder, natural briquetting grade, 99.9995% (metals basis) was purchased from Alfa Aesar. The other

---

* Corresponding author. Tel.: +86 551 3606853; fax: +86 551 3602969.
E-mail address: lfyan@ustc.edu.cn (L. Yan).

0144-8617/$ – see front matter © 2010 Elsevier Ltd. All rights reserved.
doi:10.1016/j.carbpol.2010.08.038

reagents (HAc, NaOH, $NaNO_3$, and $KMnO_4$) of analytical grade and 98% H_2SO_4, 30% H_2O_2 were purchased from Sinopharm Chemical Reagent Co. Ltd. in China and were used as received without further purification. Ultrapure water with resistivity of 18 MΩ cm was produced by a Milli-Q (Millipore, USA) and was used for solution preparation.

2.2. Preparation of graphene oxide

Graphene oxide was prepared from natural graphite by the well-known Hummers method with little modification (Becerril et al., 2008; William, Hummers, & Richard, 1958). In brief, 2 g natural graphite powder was added into a 250 mL beaker, then 1 g $NaNO_3$ and 46 mL H_2SO_4 were added into it sequentially under stirring in an ice-bath. Next, 6 g $KMnO_4$ was added slowly into the beaker under stirring and the temperature was controlled below 20 °C. The ice-bath was removed after 5 min and the system was heated at 35 °C for 30 min, and then 92 mL water was added slowly into the system and it was stirred it for another 15 min. Then 80 mL hot water with 60 °C and 3% H_2O_2 aqueous solution were added to reduce the residual $KMnO_4$ till no bubble was appeared. Finally, the system was centrifuged at 7200 rpm for 10 min, and the obtained powder was washed by warm water until the pH value of the upper layer suspension arrives at near 7. The obtained yellow-brown powder was re-dispersed into ultrapure water and was treated by mild ultrasound for 15 min, and there forms a homogeneous suspension with different concentrations after filtering the trace black residues. Graphene oxide powder was obtained after freeze drying of the suspension.

2.3. Preparation of chitosan/graphene oxide films

Highly oxidized graphene oxide, especially synthesized from natural graphite, can be easily dispersed in water. Based on this, a desired amount of graphene oxide powder (0.10–0.30 g) was dispersed into 100 mL of ultrapure water and was treated by mild ultrasound for 15 min in a 250 mL beaker, and there forms a homogeneous suspension. 1 ml HAc and 1.5 g chitosan were added into the suspension sequentially under stirring. After 60 min of stirring at room temperature, the CS and graphene oxide mixture solutions were prepared as shown in Fig. 1. The mixed solution was cast on a glass plate and a gel-like sheet with a thickness of about 0.9 mm was found, and it was kept under reduced pressure to get rid of air bubbles. The degassed product was coagulated at 50 °C for 24 h in an oven. The dry films still contained a small quantity of the HAc, and the prepared films were immersed in 0.1 M aqueous NaOH for 20 min to neutralize the acid followed by washed in ultrapure water and dried in air at room temperature for 48 h. Finally, the composite films were dried in a vacuum at 40 °C for further experiment. By changing the weight ratio of CS to graphene oxide, such as 1.5:0.1, 1.5:0.2, and 1.5:0.3, a series of CS/graphene oxide composite films coded as CS/GO-1, CS/GO-2, and CS/GO-3 were prepared. In particular, the film coded as CS-0 was prepared from pure chitosan in the acetic acid aqueous solution according to the same method. Apparently, the content of graphene oxide in the composites (chitosan and graphene oxide) were 0, 6.0, 12.0, and 18.0 wt%. The film with more than 18.0 wt% of graphene oxide was difficult to prepare due to its very high viscosity.

2.4. Characterization

To obtain information on interactions among HAc, CS, and graphene oxide, dynamic rheological analysis was performed. Tests of the rheological properties of the samples were carried out with a rheometer (Haake Mars II). Strain sweeps were run to confirm the linear viscoelastic region for each sample. The maximum resulting strain of all samples was less than 0.01.

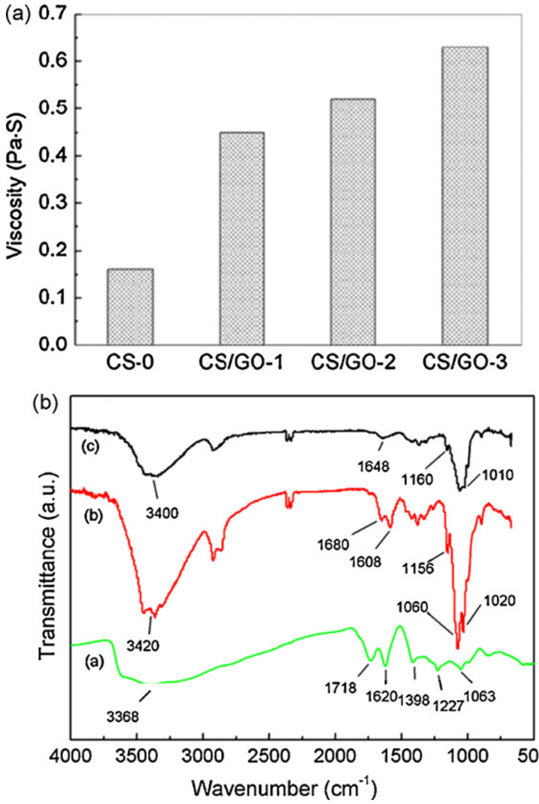

Fig. 1. (a) Rheological properties of mixtures of CS and graphene oxide: angular frequency dependence of *G*′ (solid symbols) and *G*″ (hollow symbols); (b) the FT-IR spectra for graphene oxide (curve a), CS/GO-3 (curve b), and CS-0 (curve c).

FT-IR spectroscopy was used to obtain the information about the interactions between chitosan and graphene oxide sample. FT-IR spectra were measured on a Perkin-Elmer FT-IR in the range 4000–500 cm^{-1}.

TG/DTG curves of the films were obtained by Shimadzu TGA-50 thermogravimetric instrument. The temperature range is employed from 20 to700 °C with a ramp rate of 10 °C min^{-1}.

To clarify the crystal structure of the films, wide-angle X-ray diffraction (XRD) measurements were performed on a setup with Mar 345 image plate as detector and the Cu Kα was used as the source (wavelength $\lambda = 0.1542$ nm). The recorded region of 2θ was 5–45°, and the scanning speed was 2.0° min^{-1}.

The surface structures of the films were measured using a Shimadzu SEM (Superscan SSX-550, Japan). The films were frozen in liquid nitrogen, and immediately snapped and then vacuum-dried. The fracture surfaces (cross-section) of the films were coated with gold, and then were observed. A commercial atomic force microscope (Nanoscope IIIa, Digital Instruments, Santa Barbara, CA), equipped with a J scanner, was used to measure the morphologies of the films. A silicon probe (model TESP, Nanoprobes, Digital Instruments) with a cantilever length of 125 lm and a resonant frequency of about 300 kHz was used. The scan rates were in between 0.5 and 1.0 Hz.

The tensile strength (σ_b) and elongation at break (ε_b) of the composite films were measured on a universal tensile tester (TS7104, Shenzhen SANS Test Machine, China) according to ISO527-3:1995 at a speed of 5.0 mm min^{-1}. The specimens were in rectangular shape with dimension of 20 mm × 5 mm × 0.06 mm. The length between two grips was set as 10 mm. The average values and standard deviations of the Young's modulus and tensile strength σ_{max} were evaluated for five tested specimens.

Dynamic mechanical analysis (DMA) was conducted on a dynamic mechanical analyzer (DMA-7, PerkinElmer Instruments). The measurements were performed in a nitrogen atmosphere to avoid thermal oxidation. A heating rate of 5 °C min^{-1} was applied in 1 Hz frequency for an original length of 10 mm. A tensile deformation of 0.25% was applied to the specimen.

To investigate the water-resistance, the as-prepared films with different content of graphene oxide were kept in ultrapure water until they reached the swollen equilibrium (typically about 48 h), and weighed quickly after removal of excessive water on the surface by wiping. The weighed films were dried in vacuum at 50 °C for about 48 h and reweighed. The water content in the films was defined as follows:

$$\text{water content} = \frac{W_{\text{Wet}} - W_{\text{dry}}}{W_{\text{dry}}} \times 100\%$$

where W_{wet} and W_{dry} are the weights of the wet and dry films, respectively.

Contact angles of the film samples with the water were measured by a contact angle goniometry (JC2000C, Zhongcen, Shanghai, China) at room temperature.

3. Results and discussion

Chitosan and graphene oxide can be well mixed and form homogeneously aqueous solution, and the obtained mixture is stable at room temperature. After casting the solutions of chitosan or chitosan/graphene oxide onto substrates, there form the films. The thickness of these films is 60 ± 6 μm. At the wavelength of 540 nm, the transmittance of the sample RC-0 is 90.3%. As a contrast, the transmittance of the sample CS/GO-3 decreases to 0.9%, indicates more graphene oxide adding should decrease the transmittance of the mixture film. The viscosity of the mixture increases with the adding of graphene oxide. It is well-known that dynamic rheology is a powerful tool for evaluating the structure of melts or solution. The storage modulus G' and loss modulus G'' of CS/graphene oxide suspensions are shown in Fig. 1a. From the curves of all the samples, G'' is always larger than G' over the whole frequency range, indicates a typical rheological feature of a polymer solution. In addition, the values of G' and G'' are raised up with the increasing loading of graphene oxide, and G' had larger scale increasing value, also indicating that the increasing of graphene oxide can enhance the interactions among the molecules in the solution. FT-IR studies confirm the successful oxidation of graphite to graphite oxide. The IR spectrum of our graphene oxide is similar to a previous report in the literature (Bissessur, Liu, White, & Scully, 2006). The FT-IR spectrum of graphene oxide in Fig. 1b (curve a) depicts a strong –OH peak at 3368 cm^{-1} and other C–O functionalities such as COOH (1718 cm^{-1}), C–OH (1398 cm^{-1}), and C–O–C (1063 cm^{-1}) are clearly visible. The spectrum also shows a C=C peak at 1620 cm^{-1} corresponding to the remaining sp^2 character. For chitosan, the peaks at 3400 cm^{-1} are corresponding to N–H stretching vibration, of amino group in the spectrum, shown in Fig. 1b (curve c). The absorption peaks at 1010 and 1160 cm^{-1} are attributed to primary alcoholic group of C_6–OH and secondary alcoholic group of C_3–OH. The peak at 1648 cm^{-1} is assigned to carbonyl stretching vibration of acetylated amino group. The peaks of the characteristic absorption in the curve of CS/graphene oxide are approximately similar with the curve of pristine chitosan as shown in Fig. 1b (curve b). However, the result indicates the formation of an intercalated and exfoliated structure. The FT-IR spectrum of the CS/graphene oxide compound shows a combination of characteristics similar to that of the pristine chitosan and graphene oxide which include the broad absorption band located at 3400 cm^{-1} assigned to the mixture of the amine stretch from the chitosan and to the OH groups in graphene oxide. The peak at 1680 cm^{-1} is assigned to the COOH groups from graphene oxide and is downshifted due to hydrogen bonding between the graphene oxide and hexatomic ring of the chitosan. Besides, the peak at 1608 cm^{-1} is assigned to the C=C groups from graphene oxide and is also downshifted compared to pristine graphene oxide. The peak in the region about 1060 cm^{-1} is indicative of C–O–C stretching from the graphene oxide layers. The FT-IR results indicate the existence of the interaction between chitosan and graphene oxide.

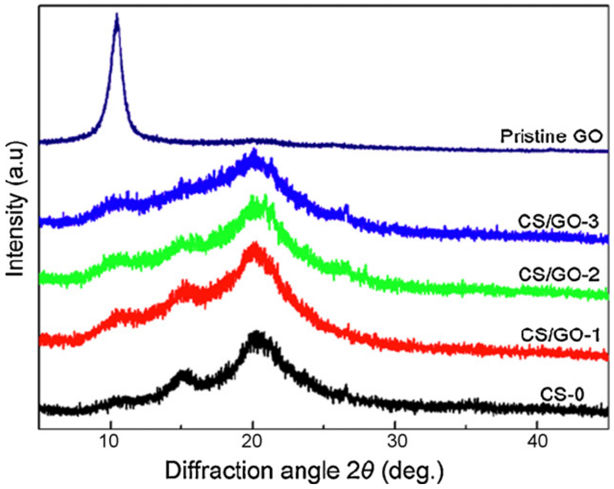

Fig. 2. XRD patterns of CS-0, CS/GO-1, CS/GO-2, CS/GO-3, and pure graphene oxide.

The XRD patterns of the films with different content of graphene oxide are shown in Fig. 2. The interlayer spacing of our synthesized graphene oxide is 0.83 nm, which is within the range of values that had been previously reported (Bissessur et al., 2006). All of the prepared films exhibit two broad peaks at $2\theta = 14.9°$ and 20.3°, due to the generally amorphous state of the chitosan films. The diffraction angles of the composite films are similar to the pure CS, and the diffraction peaks corresponding to graphite oxide has not been observed, indicates the exfoliation of them. Besides, The stronger diffraction intensity of the chitosan than that of the CS/graphene oxide composite at $2\theta = 14.9°$ imply a slightly higher crystallinity of the former than the latter, and it reveals that the crystalline degree of chitosan decrease after adding graphene oxide. However, the chemical structure of the chitosan in the composite films barely changes with the increasing content of graphene oxide, indicating that there were mainly physical interaction but scarcely chemical reaction between chitosan and graphene oxide.

SEM measurements provide direct information regarding the interfacial interactions of these composite films, as shown in Fig. 3. In Fig. 3a, the surface of the CS-0 displays some banded structures, which are attributed to the self-aggregation tendency of chitosan in solution. The surfaces of the CS/GO-1, CS/GO-2, and CS/GO-3 display a generally smooth morphology, as shown in Fig. 3b–d, indicating that the chitosan films blending with graphene oxide are miscible. For the physical cross-linking and chain entangling of the chitosan, the inner structure of CS/GO-1, CS/GO-2, and CS/GO-3 are much denser than these of CS-0, which predicts the enhancement of the tensile strength. In addition, the surface of the composite films exhibit high homogeneity, indicates the unification of chitosan and graphene oxide in the composite. The cross-sections of the composite films shows obvious grooves which were caused when the films were snapped, owing to the different structures and stiffness between chitosan and graphene oxide, as shown in Fig. 3e–h. Comparing with the pure chitosan film, the density of the blended films increase apparently, indicates the strong interaction among chitosan and graphene oxide. In addition, clear stratification appears in CS/GO-3 film. However, since the blending graphene oxide is

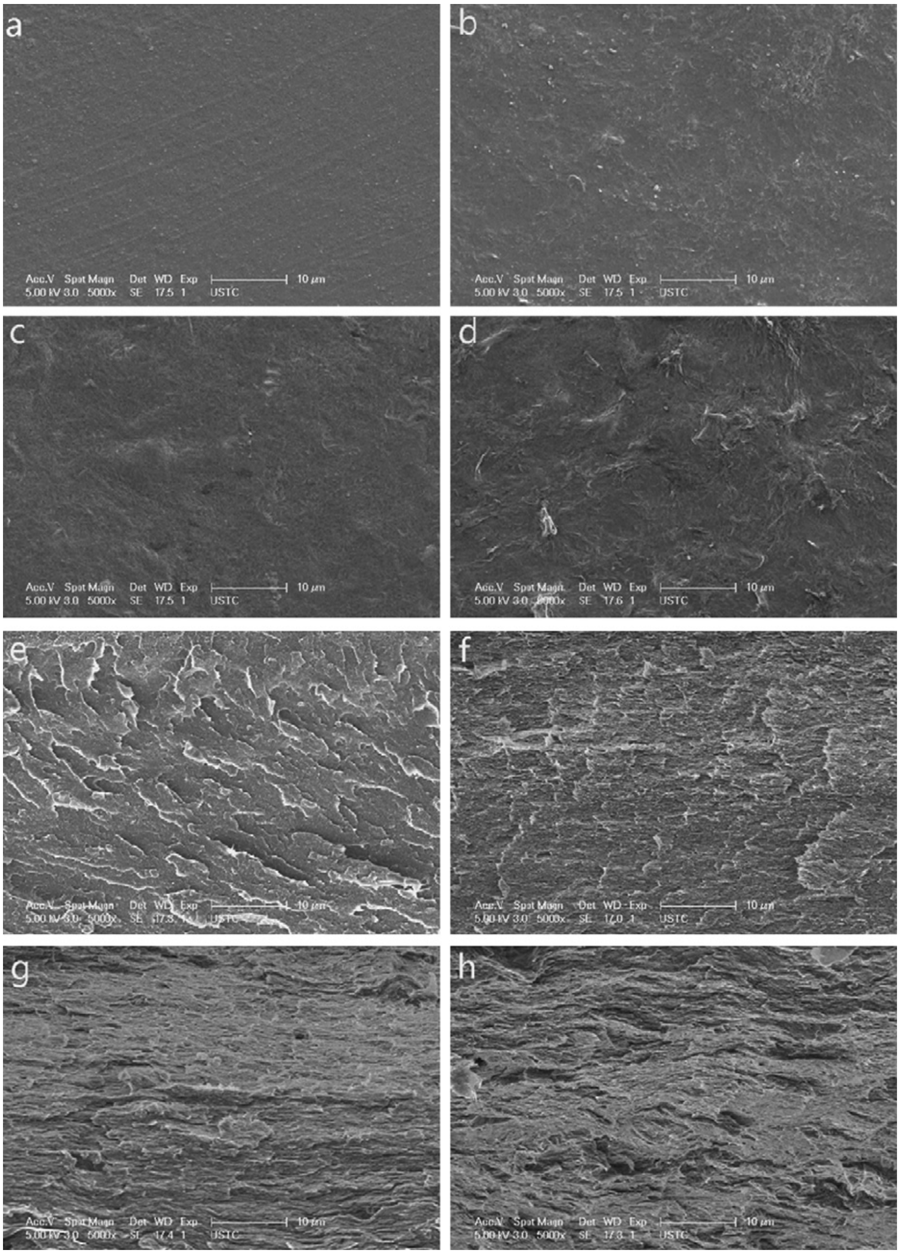

Fig. 3. SEM images of surfaces of CS-0 (a), CS/GO-1 (b), CS/GO-2 (c), and CS/GO-3 (d), and the cross-sections of CS-0 (e), CS/GO-1 (f), CS/GO-2 (g), and CS/GO-3 (h).

wrapped in or covered by a chitosan layer, there is barely an isolated fully exfoliated graphene oxide sheet, indicates a good adhesion between the chitosan and the graphene oxide.

Fig. 4 shows the C_{1s} XPS spectra of both chitosan and CS/GO-3 films. Both the curves are fitted considering the following contributions: 284.7 eV for C=C species (sp^2, peak 1), 284.8 eV for C–C (sp^3, peak 2), 286.9 eV for C–O species (peak 3) and 287.9 eV for C=O species (peak 4). Compared with the pure chitosan film, in the blend film the peak at around 284.7 eV becomes wide and the characteristic peak 2 appears for the contribution of GO. In addition, the intensity of the peak 3 of blend film increase, indicates the contribution of GO. The results reveals that GO still exist as its pristine state in the blend film.

The TG/DTG curves of the films are shown in Fig. 5. One could see that the thermal degradation of CS-0 is a little different with CS/graphene oxide under the nitrogen flows. When the temperature comes to 700 °C, the remaining solid residue of chitosan is about 47 wt%, which is less than the other CS/graphene oxide composites. The results indicate the strong interaction between the chitosan and graphene oxide, which lets to an improvement of the thermal stability of the composite films. Generally, for graphene oxide the decomposition temperature is about 200 °C due to the decomposition of labile oxygen functional groups (Chen et al., 2010). Here, the decomposition temperature of the blended film is about 300 °C, indicates the interaction between chitosan and graphene oxide.

The typical stress–strain (σ vs. ε) curves for the prepared films are presented in Fig. 6. At dry state, compared with the pure chitosan film, the tensile strength at break of the composite films increase gradually with the increasing loading of graphene oxide as shown in Fig. 6a. This suggests that the addition of graphene oxide could effectively improve the mechanical strength of the composites. Moreover, with an increase loading of graphene oxide from 6.0 to 18.0 wt%, the $\sigma_{\max}$ values sharply increases from 101.5 ± 2.3 to 137.5 ± 2.9 MPa. The strong dependence of the tensile strength on the content of graphene oxide is probably related to molecule-level

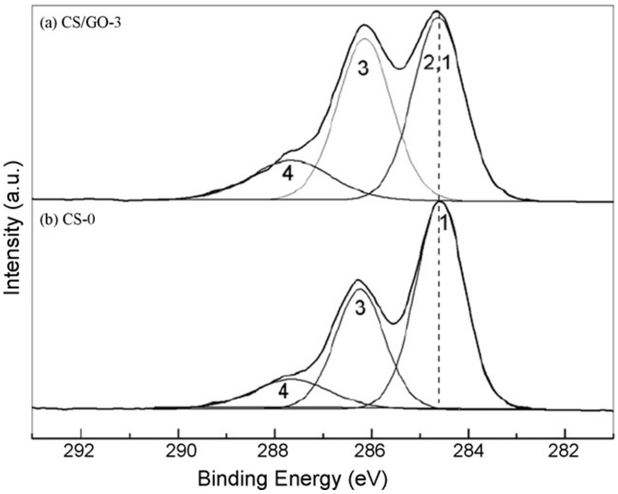

Fig. 4. C_{1s} XPS spectra of CS/GO-3 (a) and chitosan (b) films.

dispersion of graphene oxide and the strong H-bonding between the chitosan and the surface of graphene oxide. Besides, the elongations at break (ε_b) of the composite films decreases slightly on the whole compared with the pure chitosan film. Interestingly, at wet state, the tensile strength of pure chitosan decreases to merely 14.6 ± 1.4 MPa as shown in Fig. 6b. On the contrary, the tensile strength of the films blending with graphene oxide are still kept up to 43.9 ± 1.8 MPa. This reason is that water molecules interact strongly with the hydroxyl groups of chitosan, resulting in swelling and weakening of intermolecular H-bondings. With the intercalation of graphene oxide, tensile strength for the wet film significantly increase. Similarly the Young's modulus of the blended film also has a huge increase than that of pure chitosan film. The increased mechanical strength of CS/graphene oxide films at wet state is very important for their potential application as biomaterials.

Fig. 7 shows the dynamic storage modulus E' of the films are measured by DMA. Clearly, the storage moduli of all the CS/graphene oxide films are higher than that of the pure chitosan fiber, and this effect is particularly more prominent at higher temperatures. The retention ratio, defined as the ratio of the storage modulus at 180 °C to that at 25 °C, is a measure of the mechanical properties of materials with temperature. It also shows that the retention ratio increases on increasing the content of graphene oxide, and the retention ratio is only 0.63 for pure chitosan film while it reaches to 1.01 for the CS/GO-3 film. These results reveal that the CS/graphene oxide films, especially those containing more graphene oxide, possess improved mechanical properties at high temperatures.

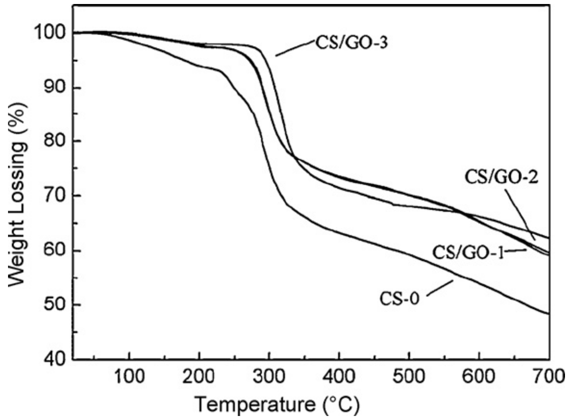

Fig. 5. TG curves of the films.

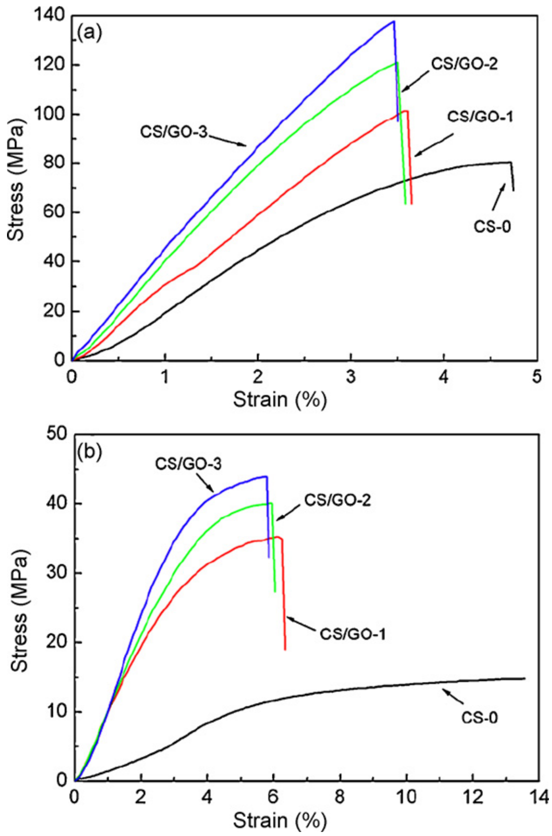

Fig. 6. Stress–strain curves of the prepared films: at dry state (a) and at wet state (b).

Comparing with the pure chitosan film, the stability of the blend film in wet environment has a hugely increasing. As shown in Fig. 8, after immersed in water for 30 days, the pure chitosan film was degraded apparently, and the film was broken and many small pieces of the film appear. However, for the blend CS/GO-3 film, there is near no degradation occurs and the film is still in a whole with strength. It reveals that blending of GO into the chitosan could increase the stability of the film, which is attracting for its potential application as packing material.

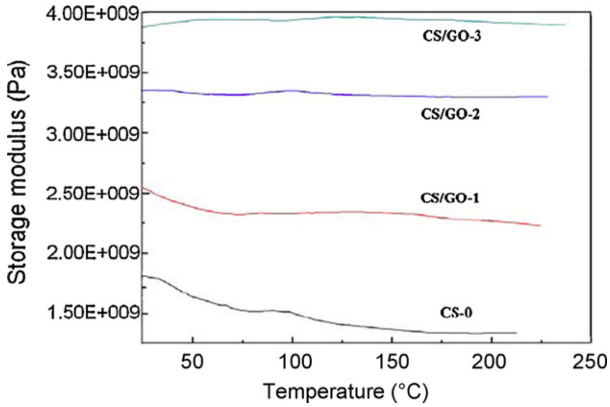

Fig. 7. Temperature dependence of the dynamic storage modulus E' of the prepared films.

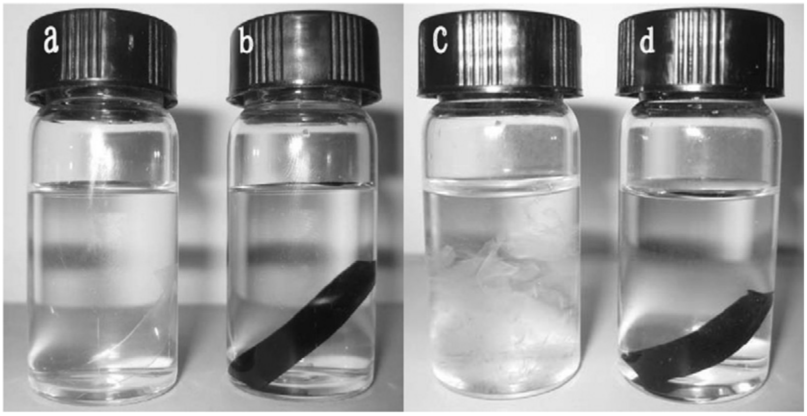

Fig. 8. Photographs of pure chitosan (a, c) and CS/GO-3 (b, d) films immersed in distilled water for 10 min (a, b) and 30 days (c, d).

4. Conclusion

Blended films of chitosan and graphene oxide have been successfully prepared by using acetic acid aqueous solution as solvent. This is a simple, low cost, and "green" pathway. The results of studies reveal the as-prepared chitosan/graphene oxide films own a certain miscibility, thermal stability and higher mechanical properties at both dry and wet state. All the results demonstrated that graphene oxide was well-dispersed in the chitosan matrix, and there are the strong H-bondings between hydroxy groups of the chitosan and hydroxy groups of the graphene oxide. In addition, the obtained composite films own higher mechanical strength than the pure RC film at high temperature. Therefore, the composite films with features of safeness, biocompatibility, and water-resistance will have promising applications as biomaterials or packing materials.

Acknowledgements

This work is supported by the National Natural Science Foundation of China (No. 20874095), the National Basic Research Program of China (No. 2010CB923302 and 2007CB210201), and the Fundamental Research Funds for the Central Universities.

References

Becerril, H. A., Mao, J., Liu, Z., Stoltenberg, R. M., Bao, Z., & Chen, Y. (2008). Evaluation of solution-processed reduced graphene oxide films as transparent conductors. *ACS Nano*, *2*(3), 463–470.

Bissessur, R., Liu, P. K. Y., White, W., & Scully, S. F. (2006). Encapsulation of polyanilines into graphite oxide. *Langmuir*, *22*(4), 1729–1734.

Chen, W. F., Yan, L. F., & Bangal, P. R. (2010). Preparation of graphene by the rapid and mild thermal reduction of graphene oxide induced by microwaves. *Carbon*, *48*(4), 1146–1152.

Coleman, J. N., Cadek, M., Blake, R., Nicolosi, V., Ryan, K. P., Belton, C., et al. (2004). High-performance nanotube-reinforced plastics: Understanding the mechanism of strength increase. *Advanced Functional Materials*, *14*(8), 791–798.

Fang, M., Wang, K. G., Lu, H. B., Yang, Y. L., & Nutt, S. (2009). Covalent polymer functionalization of graphene nanosheets and mechanical properties of composites. *Journal of Materials Chemistry*, *19*(38), 7098–7105.

Kong, B. S., Yoo, H. W., & Jung, H. T. (2009). Electrical conductivity of graphene films with a poly(allylamine hydrochloride) supporting layer. *Langmuir*, *25*(18), 11008–11013.

McAllister, M. J., Li, J. L., Adamson, D. H., Schniepp, H. C., Abdala, A. A., Liu, J., et al. (2007). Single sheet functionalized graphene by oxidation and thermal expansion of graphite. *Chemistry of Materials*, *19*(18), 4396–4404.

Niyogi, S., Bekyarova, E., Itkis, M. E., McWilliams, J. L., Hamon, M. A., & Haddon, R. C. (2006). Solution properties of graphite and graphene. *Journal of the American Chemical Society*, *128*(24), 7720–7721.

Ramanathan, T., Abdala, A. A., Stankovich, S., Dikin, D. A., Herrera-Alonso, M., Piner, R. D., et al. (2008). Functionalized graphene sheets for polymer nanocomposites. *Nature Nanotechnology*, *3*(6), 327–331.

Stankovich, S., Dikin, D. A., Dommett, G. H. B., Kohlhaas, K. M., Zimney, E. J., Stach, E. A., et al. (2006). Graphene-based composite materials. *Nature*, *442*(7100), 282–286.

Stankovich, S., Dikin, D. A., Piner, R. D., Kohlhaas, K. A., Kleinhammes, A., Jia, Y., et al. (2007). Synthesis of graphene-based nanosheets via chemical reduction of exfoliated graphite oxide. *Carbon*, *45*(7), 1558–1565.

Vickery, J. L., Patil, A. J., & Mann, S. (2009). Fabrication of graphene–polymer nanocomposites with higher-order three-dimensional architectures. *Advanced Materials*, *21*(21), 2180–2184.

Wakabayashi, K., Pierre, C., Dikin, D. A., Ruoff, R. S., Ramanathan, T., Brinson, L. C., et al. (2008). Polymer–graphite nanocomposites: Effective dispersion and major property enhancement via solid-state shear pulverization. *Macromolecules*, *41*(6), 1905–1908.

Wang, S. R., Tambraparni, M., Qiu, J. J., Tipton, J., & Dean, D. (2009). Thermal expansion of graphene composites. *Macromolecules*, *42*(14), 5251–5255.

William, S., Hummers, J., & Richard, E. (1958). Preparation of graphitic oxide. *Journal of the American Chemical Society*, *80*(6), 1339–11339.